Optimal adaptive race strategy for a Formula-E car

(Article begins on next page)

18 September 2024

Optimal Adaptive Race Strategy for a Formula-E Car

Pier Giuseppe Anselma,[a,b,*]

[a]*Department of Mechanical and Aeropsace Engineering (DIMEAS), Politecnico di Torino, 10129 Torino, Italy*

[b]*Center for Automotive Research and Sustainable Mobility (CARS), Politecnico di Torino, 10129 Torino, Italy*

Abstract

Appropriately managing battery state-of-charge and temperature while ensuring minimized lap time represents a crucial issue in Formula-E competitions. An open research question might relate to simultaneously guarantee near-optimality in the race strategy solution, computational light-weighting and effective adaptability with respect to varying and unpredictable race conditions. In this paper, a novel near-optimal real-time capable Formula-E race controller is introduced that takes inspiration from the adaptive equivalent consumption minimization strategy (A-ECMS) approach. A reduced-order Formula-E car plant model is detailed first. The optimal Formula-E race problem subsequently discussed involves controlling at each lap the depletable battery energy, the thermal management mode and the race mode in order to minimize the overall race time. Moreover, avoiding excessively depleting the battery energy and overheating the battery are considered as constraints for the race optimization problem. Dynamic programming (DP) is implemented first to obtain the global optimal Formula-E race strategy solution in an off-line control approach. The proposed real-time capable A-ECMS based race controller finds then detailed illustration. The flexibility of the introduced A-ECMS Formula-E race controller is guaranteed by optimally calibrating the related equivalence factors to adapt to the current vehicle states (i.e. battery state-of-charge, battery temperature and lap number). Simulation results for the Marrakesh e-prix considering different race scenarios in terms of battery initial temperature and Safety car entry demonstrate that the estimated race time achieved by the A-ECMS race controller is always near-optimal being 1.7% higher at most compared with the corresponding global optimal benchmark provided by DP.

___

[*] Corresponding author e-mail: pier.anselma@polito.it

1. Introduction

The paradigm shift entailed by transportation electrification currently represents a major technological challenge in the automotive industry [1][2]. As example, a large variety of forward-looking technologies has been proposed regarding vehicle drivetrain electrification and the related energy storage system and power electronics [3]-[7]. In this framework, the institution of the Formula E® race championship by the Federation Internationale de l'Automobile (FIA) in 2014 has also been aimed at further fostering these deep technological innovations [8]. Formula E® as a new motorsport category for pure electric road vehicles indeed targets not only the accelerated advancement of transportation electrification [9], but it also represents a crucial playground for the digitalization of race competitions [10].

Energy management plays a crucial role in Formula E® from the points of view of both the technological challenge and the competition between teams during races. Indeed, the energy stored in the high-voltage battery of Formula-E® race cars at the beginning of the race is limited, and each driver needs to appropriately weight its usage throughout the e-prix. As consequence, running out of battery energy before the end of the race due to poor energy management does not represent an uncommon event in Formula E® resulting in the withdrawal of the driver from the e-prix [11]. To target finishing the race in the top positions, the best trade-off thus needs to be found between the overall race time and the high-voltage battery pack preservation considering different aspects (e.g. residual energy, temperature).

In general, energy management represents a control problem for dynamic systems that can be studied with either off-line or on-line (i.e. real-time) approaches. Off-line methods exploit the knowledge of the entire dynamic scenario to be faced by the retained system to extract the optimal control trajectories over time. An example of application relates to hybrid electric vehicles (HEVs), where off-line methods can be used to identify the optimal power split between thermal engine and electric machines over time in terms of different targets (e.g. fuel economy, pollutant emission reduction) by knowing the entire driving mission in advance before running the numerical simulation [12][13]. Examples of off-line control methods include dynamic programming (DP) and Pontryagin's Minimum Principle (PMP). These approaches can be employed to perform numerical simulations and identify optimal values of design parameters for the dynamic system under consideration, or to benchmark the optimality of on-line oriented approaches. On the other hand, on-line control methods operate in real-time without knowing in advance the operational scenario and generally control the system to maximize given performance targets (e.g. energy economy, lap time) within a limited time window. They can be based as example either on heuristics (e.g. map-based, fuzzy logic) [14][15], or on instantaneous optimization [16], or on artificial intelligence [17][18].

Very few approaches have been proposed so far in literature regarding optimal race strategy and energy management applied to Formula E®. In 2020, Liu and Fotouhi used artificial neural networks to predict the performance of a Formula E® in a single lap and integrated this method in a Monte Carlo tree search algorithm to identify possible solutions as a pre-race strategy. Nevertheless, the global optimality of the identified race strategy was not validated [19]. Later, the same authors have improved their work by including a thermal model of the high-voltage battery pack. Several simulations were performed in this case in a single lap to evaluate the impact of the lap driving strategy and the usage of the attack mode on both lap time, battery energy consumption and temperature increase. However, the application of optimal control was limited to a single lap rather than to the entire race [20]. Results obtained in this last work laid the foundations for building a reducer-order numerical model of a Formula-E® car, which the same authors integrated in a deep deterministic policy gradient reinforcement learning based race strategy at the beginning of this year. A dedicated actor model was developed to handle both discrete and continuous action types, and the latter type was found particularly effective in the identification of an optimized race strategy in terms of overall time while accounting for both residual energy and temperature of the battery [21]. Despite the above cited works from Liu et al. entail a considerable advancement in the research field of optimal Formula E® race strategy, they characterize

for few key limitations and assumptions. Namely, the proposed real-time race strategies were not demonstrated identifying the global optimal race solution, e.g. they were not benchmarked with an optimal off-line controller. Moreover, probabilistic race events such as yellow flags or the entry of the Safety car following an accident as example were not extensively considered in the proposed overall race strategies. Such events may have a considerable impact on the overall race, and a proper race strategy should be able to effectively manage their eventual occurrence [22].

This paper aims therefore at overcoming the two identified research gaps and introducing a validated real-time optimal adaptive Formula E® race strategy approach considering the entry of the Safety car in a certain competition phase. To this end, a real-time control approach based on the concept of adaptive equivalent consumption minimization strategy (A-ECMS) is proposed to be applied in the field of Formula E® race strategy. An optimal calibration procedure is performed for the equivalence factors of the proposed A-ECMS by implementing a particle swarm optimization (PSO) algorithm. Moreover, a global optimal off-line control method based on DP is implemented to benchmark the performance of the A-ECMS real-time race controller. A comparison of the two control methods in different race conditions corroborates the capability of the proposed real-time strategy of returning a near-optimal race solution in terms of overall race time. The rest of this paper is organized as follows: a reduced-order plant model for the Formula E® is presented first. The optimal control problem associated to the Formula E® race strategy is subsequently discussed, and the implemented optimal off-line race strategy is detailed. The following section then aims at illustrating and optimally calibrating the proposed real-time A-ECMS based race strategy. Results are finally presented over different race conditions, and conclusions are drawn.

2. Formula-E Reduced Order Plant Model

This section aims at illustrating the considered plant model for the Formula-E® car. Particularly, the reduced-order plant model derived from Liu et al. is implemented to evaluate the lap time performance and
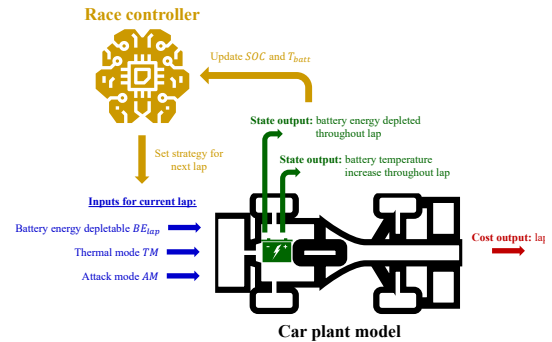

Fig. 1. Schematic diagram of the reduced-order plant model for a Formula E® car.

variations in the battery states after each single lap [21]. It should be admitted that exhaustively validating the considered reduced-order plant model with experimental data has not been possible in this paper since electric race car data from both energy and thermal perspectives are strictly proprietary of Formula E® teams. Nevertheless, the retained reduced-order plant model has been developed by Liu et al. based on accurate data generated by means of a high-fidelity Formula E® lap co-simulation platform built by interfacing IPG/Carmaker® software with MATLAB/Simulink® software. Different drive power settings, regenerative power settings, lift/coasting distance settings, and environment temperature changes were simulated to study their effects on the electric race car performance such as lap time, battery state of charge (SOC) and battery temperature. The interested reader can consult [19][20] to obtain more details regarding the development of the high-fidelity Formula E® race car plant models upon which the considered reduced-order plant model has been numerically validated.

Fig. 1 shows a schematic diagram of the reduced-order plant model and its relationship with the race controller to be developed in this paper. The plant model used in this paper refers to a second-generation Formula E® car which characterize for values of maximum tractive power and energy stored in the battery of 200kW and 52kWh, respectively [20]. Moreover, the Formula E® technical regulations allow drivers to activate the attack mode for a limited number of times throughout the e-prix. When the

Table 1

Effects of Single Lap Control Inputs on Battery States and Lap Time of Formula E® Race

States and cost Control input	SOC	T_{batt}	Lap time
BE_{lap} [1.2÷2]	$SOC(k+1) = SOC(k) - \alpha SOC_{AM} \cdot \dfrac{BE_{lap}(k)}{kWh_{batt}}$	-	$\alpha Time_{AM} \cdot f(BE_{lap}, TM)$
TM [0÷3]	-	$T_{batt}(k+1) = T_{batt}(k) + \alpha T_{AM} \cdot \mu_T \cdot 0.95^{TM}$	$\alpha Time_{AM} \cdot f(BE_{lap}, TM)$
AM [0,1,2]	$\alpha SOC_{AM} = \begin{cases} 1 & if\ AM = 0,1 \\ 1.079 & if\ AM = 2 \end{cases}$	$\alpha T_{AM} = \begin{cases} 1 & if\ AM = 0,1 \\ 1.023 & if\ AM = 2 \end{cases}$	$\alpha Time_{AM} = \begin{cases} 1 & if\ AM = 0,1 \\ 0.983 & if\ AM = 2 \end{cases}$

attack mode is activated by the driver, an extra 35kW of tractive power is made available for a limited number of laps to improve the lap performance [23].

At the beginning of each lap of the race, the controller selects the battery energy depletable throughout the single lap BE_{lap} in kilowatt-hours, a scalar value TM denoting the thermal mode which is representative of the battery thermal management, and a scalar value AM which is a flag for the usage of the attack mode. Based on values for these three control inputs, the reduced-order car plant model returns variations in battery SOC and battery temperature T_{batt} together with an estimation of the corresponding lap time. The effects of the three single lap control inputs on battery states and lap time are summarized in Table 1 and detailed as follows.

Regarding BE_{lap}, its impact on the battery SOC at each generic lap k can be evaluated following (1):

$$SOC(k+1) = SOC(k) - \alpha SOC_{AM} \cdot \frac{BE_{lap}(k)}{kWh_{batt}} \quad (1)$$

where $BE_{lap}(k)$ is the battery energy to be used in the single lap, αSOC_{AM} refers to the attack mode multiplier which will be described later in this section, and kWh_{batt} is the battery capacity in kilowatt-hours. In this car plant model, BE_{lap} is supposed not to have a direct impact on T_{batt}, while its impact on the lap time can be derived from a 2D lookup table f which reports lap time as a function of BE_{lap} and TM. This empirical table aims at modeling the lap time as a function of the driving strategy put in place by the driver for the given lap (e.g. in terms of acceleration aggressiveness, regenerative braking and 'lift and coasting' approaches), which in turn impacts on the battery

energy consumption per lap that usually ranges within 1.2kWh and 2kWh.

As concerns TM, different lap strategies to manage the battery temperature rise are modeled with a continuous variable ranging from 0 to 3. A value of 0 for TM denotes that the battery cooling system is not activated throughout the lap and the driver does not limit the driving aggressiveness or regenerative braking capability to reduce the battery temperature
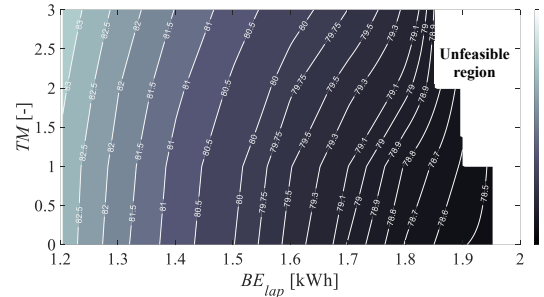

Fig. 2. Lookup table f reporting lap time as a function of selected BE_{lap} and TM for $AM = 0,1$ in the Marrakesh e-prix track.

increase. On the other hand, progressively increasing TM involves increasing the lap time while reducing the battery temperature rise by means of both the cooling system operation, the adaptation of the driving style and the regenerative braking limitation. The battery temperature after a generic lap k can thus be evaluated as:

$$T_{batt}(k+1) = T_{batt}(k) + \alpha T_{AM} \cdot T_{rise} \cdot 0.95^{TM} \quad (2)$$

where αT_{AM} and T_{rise} represent multipliers for the attack mode being used and for the reference battery

temperature increase over a single lap in the retained race, respectively. *TM* is supposed not to have a direct impact on *SOC*, while its impact on the lap time can be derived as well from the 2D lookup table *f*. In this paper, the Marrakesh e-prix track is considered, and the corresponding lookup table *f* is illustrated in Fig. 2. *f* allows predicting the lap time as a function of BE_{lap} and *TM* and it has been derived in this case from [21].

As concerns the attack mode, a value of 0 for *AM* stands for the normal mode being selected for the current lap. On the other hand, a value of 1 denotes the activation of the attack mode to enter in operation for the following lap, while a value of 2 represents the attack mode being in operation for the current lap, thus having the extra 35kW of tractive power enabled. Looking at Table 1, the attack mode being activated involves a variation in the values of the three coefficients αSOC_{AM}, αT_{AM} and $\alpha Time_{AM}$ which in turn impact on the battery SOC variation, battery temperature increase and lap time, respectively. Particularly, higher energy consumption, higher battery temperature increase and lower lap time are induced by the activation of the attack mode. It should be noted that, when the attack mode is activated, up to 2.16kWh of battery energy consumption per lap is allowed.

The highlight of the illustrated reduced-order model relates to its computational efficiency in rapidly predicting the lap time and the variation in battery states as a function of the control inputs. A competitive and demanding environment such as a live race event might therefore represent a suitable field of application for this type of modeling approach. The interested reader can consult [20] for more information regarding process to reduce the order of the considered Formula E® car plant model achieved through several higher-fidelity lap simulations.

3. Optimal Race Problem and Off-Line Strategy

In this section, the mathematical formulation for the optimal race problem in a Formula E® e-prix is discussed. Then, the global optimal solution for the retained problem is identified through the implementation of a dedicated DP based off-line optimization.

3.1. Optimal Formula-E Race Problem

The optimal control problem related to a Formula E® e-prix aims at minimizing the overall time to complete the race as follows:

$$\arg\min \left[\sum_{k=1}^{N_{lap}} lap\ time(k) \cdot \mu_{SC}(k) \right]$$

subject to:

$$SOC(N_{lap}) > 0$$
$$T_{batt}(N_{lap}) \leq T_{batt-MAX} \qquad (3)$$
$$n_{AM} \leq n_{AM-MAX}$$
$$laps_{AM} \leq laps_{AM-MAX}$$
$$BE_{lap-min} < BE_{lap} < BE_{lap-MAX}$$
$$TM_{min} < TM < TM_{MAX}$$
$$AM(k = 1,2) = 0$$

where N_{lap} represents the total number of laps for the e-prix. Values for battery SOC and temperature T_{batt} at the end of the e-prix are constrained to be respectively greater than 0 (i.e. remaining energy available to complete the race) and lower than the maximum allowed value $T_{batt-MAX}$. The total number of attack modes throughout the race n_{AM} needs to be lower than the maximum number n_{AM-MAX} allowed by regulations for the given e-prix. Similarly, for each attack mode activation, the number of laps completed in attack mode $laps_{AM}$ is required to be lower than the maximum allowed number $laps_{AM-MAX}$. As specified by the Formula E® technical regulations, activating the attack mode is not available in the first two laps of the race [23]. Finally, values for both BE_{lap} and TM need to be within the physical ranges allowed by the plant model. μ_{SC} represents a weighting coefficient that accounts for the Safety car entry throughout the race. The Safety car entry in a particular phase of the race represents an impactful event in the e-prix. Indeed, drivers are demanded to queue in a platoon that proceeds at slow speed for few laps before getting back to the normal race. In this case, gaining distance from the drivers behind in the initial phases of the e-prix by reducing the average lap time (and consequently depleting and heating the battery more) might be neutralized when platooning behind the Safety car. On the other hand, a beneficial condition may relate to have large residual energy and low

battery temperature when getting back to the normal race after the exit of the Safety car. To include this consideration in the mathematical formulation of the Formula E® race problem, assuming one Safety car entry occurring throughout the retained e-prix, a value of μ_{SC} lower than 1 is considered for the laps performed before the Safety car entry, while a value of μ_{SC} equal to 1 is retained for the laps completed after the Safety car entry. This allows giving more emphasis to the laps to be completed when getting back to the normal race as the Safety car exits.

For the laps in which the racing cars need to travel behind the Safety car, the lap time is kept constantly to 112.91s as it can be obtained by increasing by 40% the average lap time in Fig. 2 as suggested in [24]. As concerns the battery temperature, a cooling rate of 0.952° C per lap is supposed as it can be derived from the results over time for the simulations of a Formula E® car travelling behind the Safety car in the Marrakesh e-prix shown in [19]. Other than battery cooling, slow driving behind the Safety car involves limiting the battery energy consumption: only 0.23kWh per lap are indeed required by interpolating the BE_{lap} curve at TM equal to 0 and 112.91s of lap time. However, to stimulate the competition and advance the development of dedicated race strategies, the Formula E® technical regulations impose a 1kWh deduction of available battery energy applied to each driver per minute of each Safety car period [23]. For a lap time corresponding to 112.91s, this results in an equivalent battery energy consumption of 2.11kWh per lap in which the Safety car is on track.

The control variable set U associated to the illustrated control problem is reported in (4) and values for each of the three variables contained need to be decided at the beginning of each lap.

$$U = \begin{Bmatrix} BE_{lap} \\ TM \\ AM \end{Bmatrix} \qquad (4)$$

U includes the battery energy depletable, the thermal management mode and the attack mode to be set at the beginning of each lap, as illustrated in Fig. 1. Variables contained in U in turn impact on the battery states and the race cost function as recalled in Table 1. A global optimal off-line approach for solving the illustrated race control problem will be detailed in the follow-up of this section.

3.2. Global Optimal Off-line Race Strategy

In this paper, DP is implemented first as an off-line algorithm that can identify the global optimal solution for the race problem detailed above. DP represents a widely implemented approach to evaluate global optimal solutions for dynamic control problems [25]-[27]. Based on the Bellman's principle of optimality, DP can find the global optimal solution by exhaustively searching through discretized control variables and state variables for the retained control problem. The optimal solution can thus be identified by minimizing the overall value of cost function for the entire dynamic problem [28]-[31]. In DP, the set of state variables needs definition that contains the physical variables to be tracked throughout the dynamic problem (i.e. the Formula E® race). Evaluating the evolution over time of state variables and imposing constraints on their punctual and final values is allowed in this way [32]. Four state variables are included in X to be associated with the Formula E® race problem under analysis as reported in (5).

$$X = \begin{Bmatrix} SOC \\ T_{batt} \\ AM \\ laps_{AM} \end{Bmatrix} \qquad (5)$$

Evaluating the evolution of SOC and T_{batt} throughout the race allows constraining their final value to be within the physical allowed limits (i.e. greater than 0 for SOC and lower than $T_{batt-MAX}$, for T_{batt}, respectively). Including AM is performed for two main reasons. First, it allows ensuring that an activation lap (i.e. AM=1) is achieved before entering the actual attack mode (i.e. AM=2). Moreover, it allows detecting each mode attack activation to make sure that the DP controller does not overcome the maximum allowed number n_{AM-MAX}. Finally, the number of laps driven in attack mode for each attack mode activation is accounted in order to comply with $laps_{AM-MAX}$.

In this work, the DP function implemented in Matlab© software and made available by Sundstrom and Guzzella is used [33]. The Marrakesh e-prix track is retained, a value of 2 is considered for both $laps_{AM-MAX}$ and n_{AM-MAX}, while the maximum temperature achievable by the battery is set to 58° C as suggested in [21]. As stated by the Formula E®

(a) Estimated race time
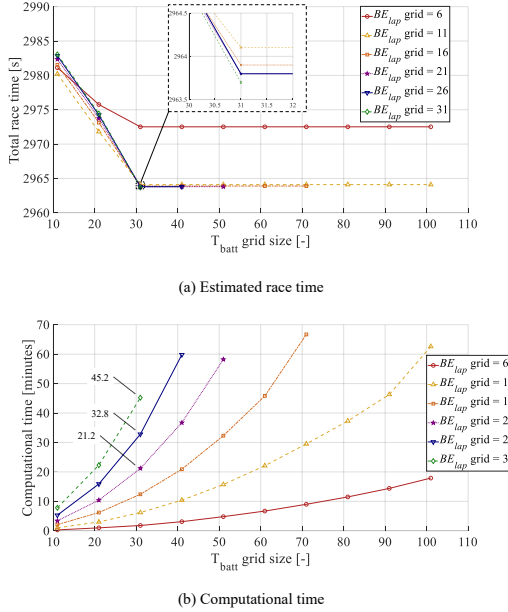

(b) Computational time

Fig. 3. Sensitivity results for the DP mesh sizes in terms of ERT and CT.

technical regulations, each race lasts 45 minutes. Once the 45 minutes are up and the leader has crossed the finish line, a supplementary final lap needs to be completed [34]. For the Marrakesh e-prix, the total number of laps thus amounts to 35 in this case considering 34 laps achievable in the 45-minute span and the additional final lap. The initial battery temperature is assumed being equal to the ambient temperature, with a value of 30° C assumed in this DP case study. Moreover, it is assumed that, for this initial case study, the Safety car enters the track at the beginning of lap 15 and leaves it at the end of lap 17. Considering these input data, a sensitivity analysis is performed in this sub-section to determine the most suitable grid sizes to be retained for control and state variables in DP when solving the optimal race problem under analysis. In particular, the mesh for the control variable BE_{lap} is discretized with [6, 11, 16, 21, 26, 31] elements, while the corresponding state variable SOC is discretized with 10 times the number of elements compared with BE_{lap}. As concerns T_{batt}, the corresponding state variable is discretized with [11, 21, 31, 41, 51, 61, 71, 81, 91, 101] elements. Finally, the discretization of TM is performed considering a

number of elements equal to rounding-up the size of T_{batt} divided by 5. An odd number of elements is considered for the discretized vectors of state and control variables in order to take into account the middle values of each variable for all the discretization options.

Results obtained for the sensitivity analysis considering DP are reported in Fig. 3 both in terms of estimated race time (ERT) and computational time (CT). ERTs can be directly evaluated from the solution obtained from DP for the considered optimal race control problem, while CTs in this case refer to a desktop computer with Intel Core i7-8700 (3.2 GHz) and 32 GB of RAM. Only the results corresponding to sizes of the sensitivity variables allowed by the computational capability of the employed desktop computer in terms of processing and storage memory have been reported. As regards T_{batt}, a knee-point for the ERT can be observed in Fig. 3(a) for 31 elements in the corresponding state variable for all the BE_{lap} grid sizes. Observing a knee-point in the optimality of the solutions is common within sensitivity analysis of DP [13]. 31 elements are thus suggested being considered in the T_{batt} state variable, since a higher number of elements would increase the corresponding CT without further improving the optimality of the DP solution. As concerns BE_{lap}, progressive reduction in the ERT can be observed in Fig. 3 (a) for 31 elements of T_{batt} when increasing the size of BE_{lap} up to 21 elements. However, when further increasing the number of elements for BE_{lap} beyond 21, little advantage is obtained in terms of optimality of ERT, while the corresponding CT is observed remarkably increasing in Fig. 3(b) from 21.2 minutes up to 45.2 minutes. In this case, limiting the grid size for BE_{lap} to 21 elements might be suggested as a reasonable trade-off between optimality of the ERT solution and corresponding computational cost.

4. Real-time Optimal Race Strategy

The mathematical formulation for the optimal Formula E® race problem and the related off-line control algorithm have been described in the previous section. Even though the off-line control achieved by implementing DP can return the global optimal solution for the energy management problem in a

Formula E® e-prix, the achievement of this approach appears difficult in a real-world race scenario. A first limitation in this framework relates to the computational cost. Indeed, 21.2 minutes are required to complete the DP workflow for the optimal race problem under analysis. This might contrast with a race environment in which control decisions need to be achieved within few seconds. A second drawback concerns DP requiring the full knowledge of the race events a priori, namely the given laps in which the Safety car will be on track in this case, which cannot be known beforehand in a real-world scenario. To overcome this drawback, this section aims at describing a real-time capable Formula E® race strategy based on the widely employed A-ECMS control approach. The implemented A-ECMS

approach is presented first, followed by the calibration of the values of equivalence factors through the implementation of a PSO algorithm.

4.1. A-ECMS Race Strategy for Formula-E

ECMS was introduced as control approach by Paganelli and by Delprat in 2002 [35][36]. It represents a real-time implementation of the Pontryagin's minimum principle, and it was originally derived from the optimal control theory applied to the field of hybrid electric vehicles and presented by Delprat in 2001 [37][38]. The key principle of ECMS, when applied to hybrid electric powertrains, is that an equivalent fuel consumption can be related to the use electrical energy. An instantaneous cost function can
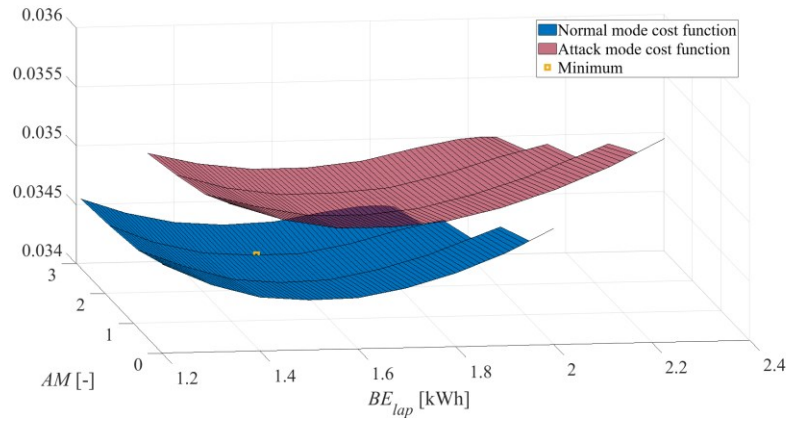
(a) $s_{SOC} = 0.12$; $s_t = 0.08$
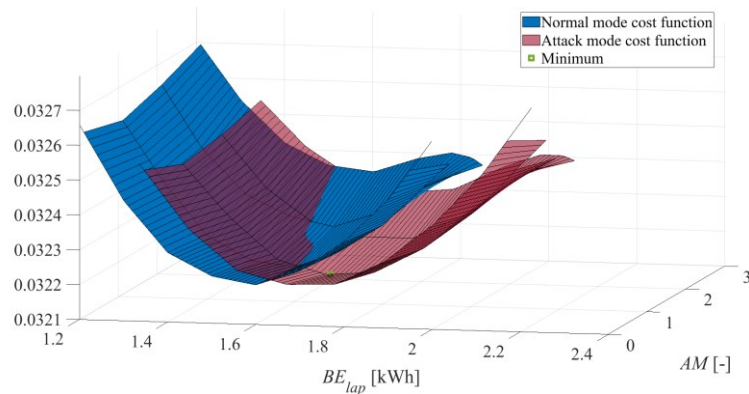
(b) $s_{SOC} = 0.10$; $s_t = 0.03$

Fig. 4. Cost functions for normal mode and attack mode as a function of control variables BE_{lap} and TM for different values of equivalence factors.

be evaluated as the sum of the two energy contributions (fuel and electricity), weighted by means of a dedicated equivalence factor s [39]. The control decision is achieved at each time instant by setting values of control variables corresponding to the minimum of the cost function [40]. The equivalence factor s is kept as constant in the traditional version of ECMS, while it is varied over time in the A-ECMS. An A-ECMS approach for hybrid electric powertrains was initially proposed by Musardo et al. in 2004 by adapting s over time according to the current value of battery SOC, paving the way for copious similar approaches developed in the following decade [41]-[44].

In this work, the cost function J_{A-ECMS} that needs minimization at each lap k in A-ECMS is reported in (6) and involves lap time, battery energy consumption and battery temperature increase:

$$J_{A-ECMS}(k) = [1 - s_{SOC}(SOC, T_{batt}, k)]$$
$$\cdot [1 - s_T(SOC, T_{batt}, k)]$$
$$\cdot lap\ time(k)$$
$$+ s_{SOC}(SOC, T_{batt}, k)$$
$$\cdot \Delta_{SOC}(k) + s_T(SOC, T_{batt}, k)$$
$$\cdot \Delta_{Tbatt-rel}(k) \qquad (6)$$

with:

$$\Delta_{Tbatt-rel}(k) = \frac{\Delta_{Tbatt}(k)}{T_{batt-MAX} - T_{Batt}(0)}$$

where s_{SOC} and s_T represent two equivalence factors for the use of battery energy and the increase in battery temperature, respectively. These are not constant, rather they are updated at the end of each lap k based on the battery SOC, the battery temperature and the lap number k. Δ_{SOC} is the estimated variation in battery SOC for the current lap according to the selected values of control variables (i.e. BE_{lap}, TM and AM). Similarly, $\Delta_{Tbatt-rel}$ is the relative variation in battery temperature for the current lap, and it depends on the battery temperature variation Δ_{Tbatt} at the end of the given lap k normalized according to the maximum battery temperature variation allowed throughout the race.

By increasing the values of s_{SOC} and s_T it becomes possible in this way to progressively limit the battery energy depletion and the battery temperature increase at the expense of an increase in the lap time. At the
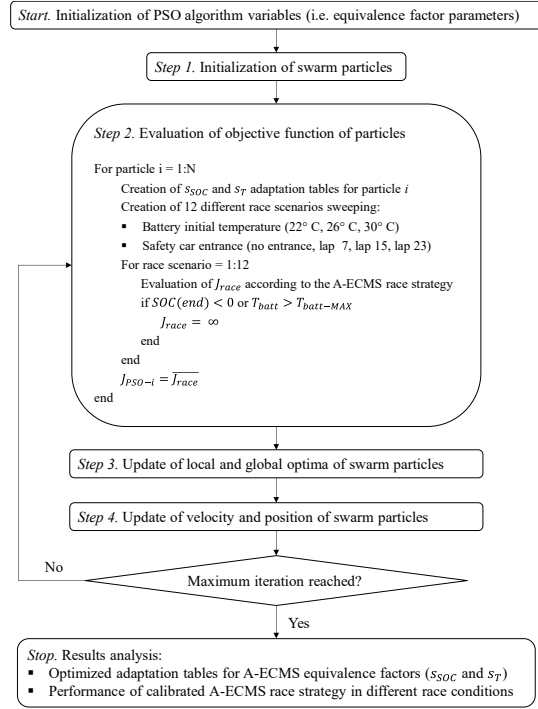

Fig. 5. Flowchart of the implemented PSO algorithm for optimal calibration of the A-ECMS equivalence factor.

beginning of each lap, two cost functions are particularly evaluated for the normal mode and the attack mode, respectively. If the minimum for the cost function associated to the attack mode is lower than the minimum for the cost function associated to the normal mode, the value of AM for the corresponding lap is set to 1 and the attack mode is set to be in operation in the following lap. Fig. 4 illustrates examples of response surfaces for cost functions associated to both normal mode and attack mode obtained from the reduced-order Formula E® car plant model as a function of control variables BE_{lap} and TM for different values of equivalence factors. For values of equivalence factors associated to Fig. 4(a), the minimum belongs to the response surface associated to the cost function of the normal mode, which would therefore be selected as operating mode for the given lap. On the other hand, when modifying the values of equivalence factors as linked to Fig. 4(b), the minimum belongs to the response surface for the attack mode cost function, this latter becoming thus advantageous in turn.

As a common practice, particular attention should be paid to the calibration of the equivalence factors in the A-ECMS. This indeed represents a crucial step that might notably affect the optimality of the control solution produced by A-ECMS, as it can be already observed in the modifications in the response surfaces for the cost functions in Fig. 4(a) and Fig. 4(b).

4.2. Optimal Calibration of the Equivalence Factors

In the formulation of the A-ECMS provided in the previous sub-section, values for both s_{SOC} and s_T need to be defined as a function of *SOC*, T_{batt} and lap number in the form of 3D lookup tables. In this work, s_{SOC} and s_T are retained to linearly increase for progressively increasing values of *SOC*, T_{batt} and lap number. In this work, ranges of *SOC*, T_{batt} and lap number are particularly discretized with five elements each from the lowest to the highest possible value. Intermediate values of equivalence factors can then be obtained by linearly interpolating within the discretized values. Considering five discretized values for each of the three variables affecting the equivalence factors leads to retain $5^3=125$ different values to be calibrated for each equivalence factor, thus 250 parameters in total. The consideration of five discretized elements of equivalence factors with respect to the values of both *SOC*, T_{batt} and lap number stems from seeking a trade-off between control accuracy and computational cost. Indeed, further increasing the number of elements would lead to exponentially increase the number of equivalence factor parameters to be tuned within the calibration process (e.g. 432 parameters to be calibrated for four discretized elements, 686 parameters to be calibrated for five discretized elements).

The calibration of the discretized adaptation tables for s_{SOC} and s_T represents in this case a further optimization problem considering 250 variables. In this framework, an efficient approach requires implementation to explore the 250-dimensional calibration space, since operating an exhaustive search may result unpractical. To this end, PSO is implemented in this paper as a well-known approach for solving global optimization problems. PSO is an iterative stochastic optimization algorithm that relies on a numerical model capturing the social behavior of fishes and birds proposed by Kennedy and Eberhart in 1995 [45]. The flowchart of the PSO approach implemented in this work is illustrated in Fig. 5 and detailed as follows. During step 1, a population of N particles is initialized aiming at the subsequent exploration of the calibration space searching for the minimum of the PSO cost function J_{PSO}. At each iteration of the PSO algorithm, step 2 aims at assessing the value of J_{PSO} for each particle of the swarm. This is performed by simulating the Formulae E® car reduced-order plant model presented in section II being controlled by A-ECMS in the Marrakesh e-prix considering the equivalence factor adaptation tables corresponding to the given swarm particle *i*. Various race conditions in terms of initial battery temperature and Safety car entry are considered in this step for the sake of enhancing the robustness of the calibrated A-ECMS with respect to the variety of possible race circumstances. Three different values of initial battery temperature are considered corresponding to 22°C, 26° C and 30° C, and four possibilities for the Safety car entry are retained in lap 7, lap 15, and lap 23 potentially and reasonably relating to initial phase, middle phase and final phase of the race, respectively. As the safety car enters, this is assumed staying on the track for three laps, since this number relates to the highest empirical probability for a safety car phase duration as observed in [24]. The fourth Safety car case corresponds to not have it entering the track throughout the entire race. Combining initial battery temperature and Safety car entry options, totally twelve race scenarios are generated for simulating the e-prix with the Formula E® car reduced-order plant model being controlled by the proposed A-ECMS approach considering the equivalence factor adaptation tables related to the given particle *i*. For a given race scenario, if the A-ECMS that considers the calibration of s_{SOC} and s_T according to the parameters of particle *i* allows ending the simulated e-prix without excessively depleting the battery energy and overtaking $T_{batt-MAX}$, the corresponding J_{race} is retained. On the other hand, it the final battery SOC or battery temperature requirements are not met for the race scenario under consideration, the corresponding J_{race} is labelled with a remarkably large value (representative of infinite). Finally, the cost function J_{PSO-i} for the given particle *i* is evaluated as the average of the values of J_{race} evaluated over the twelve considered race scenarios. On average, only 0.5

Table 2

PSO parameters for equivalence factor adaptation tables

Category	Parameter	Value
A-ECMS equivalence factors	SOC discretization [-]	[0, 0.25, 0.5, 0.75, 1]
	T_{batt} discretization [°C]	[20, 29.5, 39, 48.5, 58]
	Lap number discretization [-]	[1, 9, 18, 27, 35]
PSO parameters	Number of variables [-]	250
	Swarm size [-]	5000
	Inertia coefficient [-]	1
	Cognitive coefficient [-]	5
	Social coefficient [-]	2
	Maximum number of iterations [-]	25

seconds are required to simulate the Formula E® car reduced-order plant model being controlled by A-ECMS in the twelve retained race scenarios on the same computational platform introduced for DP in the previous section. This suggests the computational lightweight of A-ECMS and the subsequent ease of real-time application of such approach in real-world race scenarios. Once J_{PSO} has been evaluated for all the particles of the swarm, step 3 aims at updating the local and global minima for the swarm. Position and velocity of each particle in the 250-dimensional calibration space considered are then updated in step 4 based on the local and global optima previously identified. Three main PSO parameters are involved in this procedure, namely the inertia parameter, the cognitive parameter, and the social parameter [46]. More details regarding this step can be found in [47].

Once the maximum number of iterations is reached for the PSO algorithm, obtained results include the calibrated tables for s_{SOC} and s_T as a function of *SOC*, T_{batt} and lap number, and the simulation of the Formula E® car reduced-order plant model being controlled by A-ECMS for the retained race scenarios. Compared with other popular stochastic optimization algorithms (e.g. genetic algorithm – GA), PSO distinguishes by ease of management and parameter tuning [48][49]. This corroborates the likelihood of effectively finding a global optimum for the considered calibration problem and it represents the main motivation behind the use of PSO in this work. The version of the PSO

algorithm considered in this paper refers to the corresponding toolbox provided by the Yarpiz project and it is implemented in MATLAB© software [50].

Retained PSO parameters in this work are reported in Table 2. Particularly, the five discrete values respectively considered for *SOC*, T_{batt} and lap number are illustrated, along with set values for PSO parameters. Values of inertia, cognitive and social coefficients for the PSO have been retained from [46]. A further trial-and-error check has been performed to ensure that the effectiveness of the PSO workflow could not be improved by considering different values of parameters in Table 2. Fig. 6 illustrates the trend of the best value of J_{PSO} for the entire swarm as a function of the iteration of the PSO algorithm. The optimization procedure is particularly found converging to a minimum in the retained 250-dimensional A-ECMS calibration space after the 16th iteration of the PSO algorithm. The convergence for the optimization procedure observed in Fig. 6 may suggest the effectiveness of the values of PSO parameters retained in Table 2. Extracts of the adaptation tables for s_{SOC} and s_T corresponding to the optimization-based calibration results automatically identified by PSO are shown in Fig. 7 for three different values of T_{batt}. In this case, the 2D lookup tables with lap number and SOC as independent variables for intermediate values of T_{batt} can be obtained by linearly interpolating within the two lookup tables corresponding to the adjacent discrete T_{batt} values. The squared markers in Fig. 7 represent the discretization of SOC and lap number performed for both the A-ECMS equivalence factors considered.
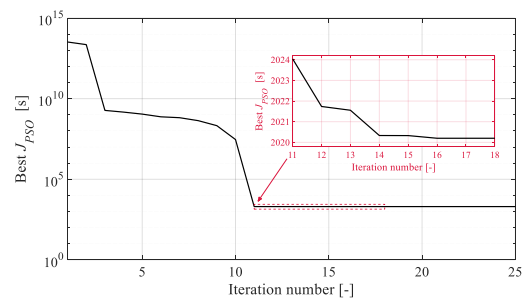

Fig. 6. Flowchart of the implemented PSO algorithm for optimal calibration of the A-ECMS equivalence factor.
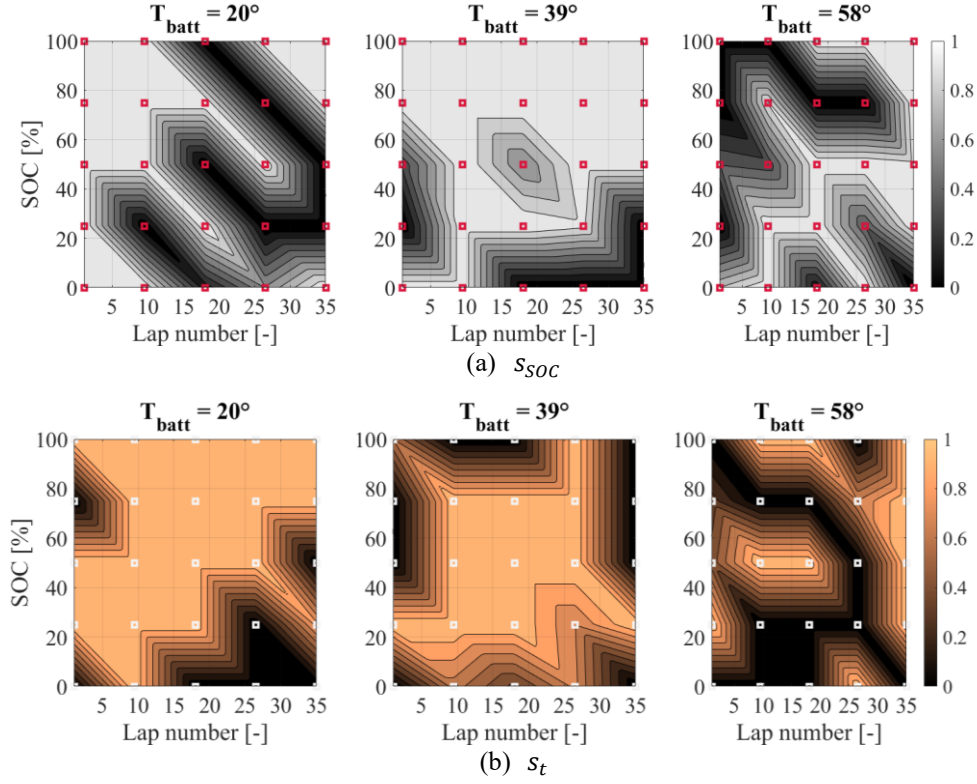
(a) s_{SOC}

(b) s_t

Fig. 7. Adaptation tables for s_{SOC} and s_T obtained from the PSO automatic calibration procedure.

5. Results

In this section, results obtained in different race scenarios of the Marrakesh e-prix are presented for both DP and A-ECMS race strategies. As mentioned earlier, the application of DP in a real-world race scenario might result unpractical due to both its off-line nature and the associated computational cost. However, as a common practice, an off-line global optimal control approach such as DP can be used to benchmark the optimality of the solutions provided by a real-time capable controller such as A-ECMS [51][52]. To this end, Table 3 reports ERTs in the twelve retained Marrakesh race scenarios for both DP

Table 3

ERTs obtained by DP and A-ECMS in the Marrakesh e-prix for different race scenarios

Initial T_{batt} [° C]	No safety car		Safety car in lap 7 to lap 9		Safety car in lap 15 to lap 17		Safety car in lap 23 to lap 25	
	DP	A-ECMS	DP	A-ECMS	DP	A-ECMS	DP	A-ECMS
22	2810.0 s	2856.7 s (+1.7%)	2918.9 s	2943.7 s (+0.8%)	2924.8 s	2943.7 s (+0.6%)	2938.4 s	2952.8 s (+0.5%)
26	2812.5 s	2850.3 s (+1.3%)	2918.4 s	2939.6 s (+0.7%)	2926.4 s	2939.1 s (+0.4%)	2939.0 s	2949.6 s (+0.4%)
30	2818.7 s	2857.7 s (+1.4%)	2916.8 s	2941.4 s (+0.8%)	2924.1 s	2941.4 s (+0.6%)	2935.4 s	2953.6 s (+0.6%)

and A-ECMS. The percentages of the difference in ERTs between A-ECMS and DP are illustrated as well. The near-optimality of the proposed version of A-ECMS can be demonstrated in this way by the corresponding ERTs being higher than the related DP ERTs by no more than 1.7% only. In general, the effectiveness of the introduced A-ECMS as Formula E® race strategy seems enhanced in the e-prix scenarios involving Safety car entry, with the corresponding increase in ERTs being always contained within 0.8% compared with the related global optimal race solution. These results are in line with the general near-optimality of the solutions provided by appropriately calibrated ECMS based controllers, as it has been already demonstrated in literature for other fields of application [42][52].

In fig. 8, a comparison is illustrated between DP and A-ECMS in terms of control actions generated and resulting lap time and car states as a function of lap number for initial T_{batt} equal to 26° C and Safety car on track from lap 7 to lap 9. In general, DP tends to set
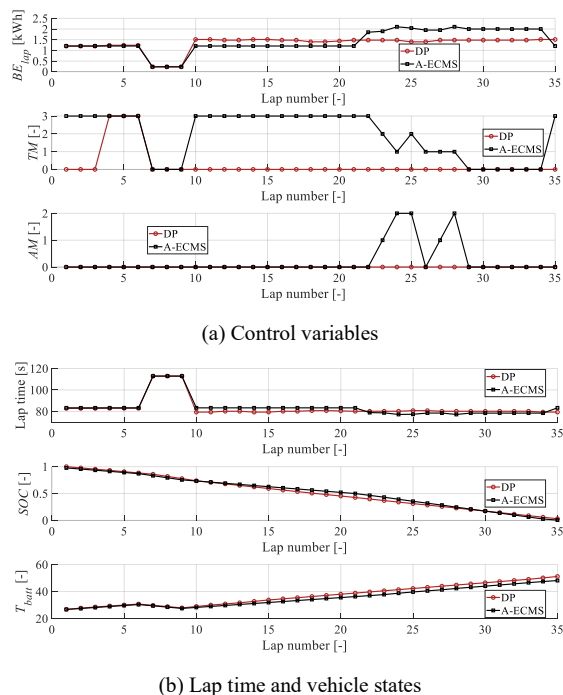

(a) Control variables

(b) Lap time and vehicle states

Fig. 8. Selected values of control variables, lap time and Formula E® car states as a function of lap number for both DP and A-ECMS (initial T_{batt}= 26° C, safety car in lap 7 to lap 9).

quite constant values of control variables in terms of BE_{lap} and TM over the simulated e-prix. Moreover, the attack mode does not find activation. This generally stems from the a priori knowledge of the entire Formula E® race scenario that allows DP to set smooth and constant control actions throughout the race. On the other hand, the control behavior of the calibrated A-ECMS varies considerably according to the specific phase of the race. In particular, a conservative strategy is performed in the initial phase of the race (e.g. up to lap number 21) both in terms of battery energy usage and battery temperature increase. Differently, the A-ECMS tends to control the Formula E® car more aggressively in the final phase of the race. This correlates with the A-ECMS setting higher values of BE_{lap} (i.e. around 2 kWh), lower values of TM (i.e. closer to 0) and activating the attack mode twice from lap number 22 onwards in Fig. 8(a). The control decisions performed by A-ECMS might relate to its real-time operation which does not involve knowing the race conditions in advance. Nevertheless, the race strategy operated by A-ECMS correlates well with a real-world e-prix scenario in which drivers need to raise the race pace in the final phases aiming at achieving the top positions. In this framework, a strategic hint might relate to activating the attack mode in the final phases of the e-prix as performed by A-ECMS in Fig. 8(a). This contrasts with the attack mode activation being performed in the first laps of the e-prix as in [21]. Indeed, an eventual Safety car entry leading the drivers to queue in a slow speed platoon might nullify the time advantage achieved earlier in the race at the expenses of lowering both the battery available energy and the allowed margin in battery temperature increase.

Fig. 9, Fig. 10, and Fig. 11 show comparisons between DP and A-ECMS in terms of control actions, lap time and Formula E® car states for initial T_{batt} equal to 26° C and Safety car on track from lap 15 to lap 17, from lap 23 to lap 25, and without safety car entry, respectively. These three figures aim at corroborating the effectiveness of the proposed A-ECMS approach in adapting to different race conditions (e.g. Safety car entry). Particularly, the A-ECMS conservative race behavior in the initial phases of the e-prix and the subsequent more aggressive race pace (e.g. after the Safety car exit) are confirmed for different race scenarios both in Fig. 9, in Fig. 10 and

14

in Fig. 11. This validates the effective adaptability of the proposed A-ECMS Formula E® race strategy approach to different e-prix scenarios. For the sake of briefness, time series obtained considering initial T_{batt} equal to 22° C and 30° C have not been plotted in figures, but the reader can refer to Table 3 for obtained results in terms of ERT for both DP and A-ECMS in these race conditions.

6. Conclusions

An optimal Formula E® race strategy is fundamental in minimizing the overall race time while preserving the battery states both from SOC and temperature points of view. The optimality of formula E® race strategies currently proposed in literature has generally not been demonstrated. Moreover, their adaptability with respect to varying and uncertain race conditions has not yet been enhanced. To answer these
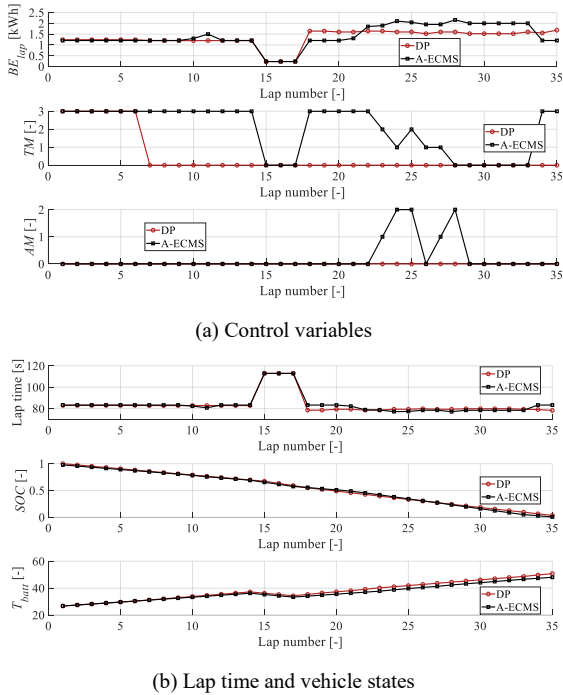

(a) Control variables

(b) Lap time and vehicle states

Fig. 9. Selected values of control variables, lap time and Formula E® car states as a function of lap number for both DP and A-ECMS (initial T_{batt}= 26° C, safety car in lap 15 to lap 17).

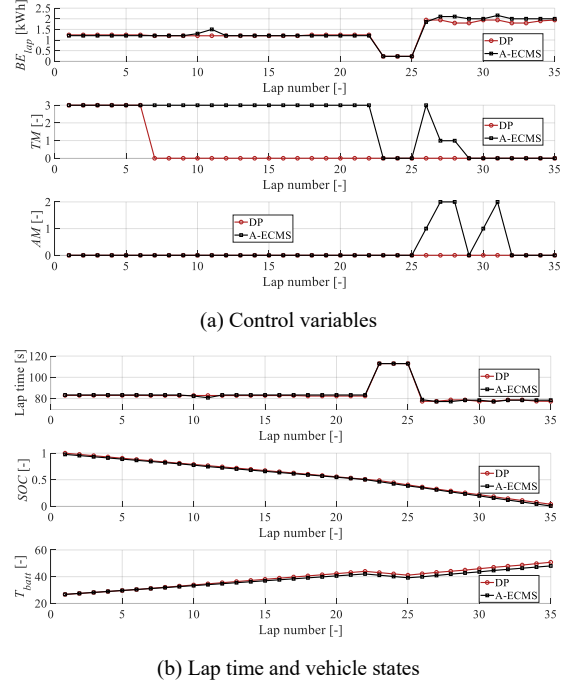

(a) Control variables

(b) Lap time and vehicle states

Fig. 10. Selected values of control variables, lap time and Formula E® car states as a function of lap number for both DP and A-ECMS (initial T_{batt}= 26° C, safety car in lap 23 to lap 25).

needs, this paper proposes a near-optimal real-time capable adaptive race strategy for a Formula E® car.

A reduced-order plant model has been presented first that allows rapidly estimating the lap time and the variations in vehicle states for a Formula E® car after a given lap of the e-prix as a function of selected control variable values. Control variables handled by the high-level race controller include the battery energy depletable throughout the lap, the thermal management mode, and the race mode (i.e. normal mode or attack mode). The optimal race problem has then been introduced and the related global optimal solution has been obtained with an off-line global optimal control approach such as DP considering the Marrakesh e-prix. The subsequent introduction of a real-time Formula E® race controller based on the A-ECMS approach has aimed at overcoming the limits in the real-world applicability of DP. The key idea supporting the proposed A-ECMS for Formula E® race management is to adapt the value of the equivalence factor as function of the current lap number, battery SOC and battery temperature. In this
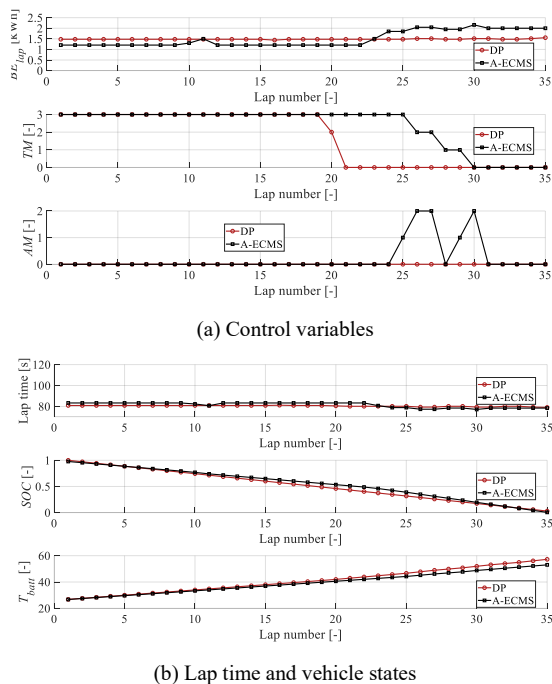
(a) Control variables

(b) Lap time and vehicle states

Fig. 11. Selected values of control variables, lap time and Formula E® car states as a function of lap number for both DP and A-ECMS (initial T_{batt}= 26° C, no safety car entry).

framework, PSO has been implemented to extract optimal adaptation tables for the A-ECMS equivalence factors. Simulation results considering different race conditions in terms of battery initial temperature and Safety car entry for the Marrakesh e-prix have suggested the near-optimality of the proposed A-ECMS Formula E® controller. In particular, the increase in ERT for the Formula E® A-ECMS race strategy is always contained within 1.7% compared with the corresponding global optimum benchmark provided by DP. Moreover, the effective adaptability of the proposed A-ECMS Formula E® race controller has been suggested by the achievement of near-optimality in ERT over different race scenarios. Effectively benchmarking the A-ECMS results with the off-line optimization results identified by DP thus provides a first validation of the near-optimality of the proposed Formula E® race strategy.

The proposed methodology is generalized and can be applied to any Formula E® racing car to minimize the overall race time while complying with battery energy and thermal constraints in real-time during an

e-prix. To apply the methodology to other formula E® cars, high-fidelity simulations need to be performed or experimental data need to be collected for characterizing the behavior of the considered car throughout a lap in a given track. Then, the considered reduced-order car plant model should be fit to numerical or experimental results. Finally, the introduced real-time Formula E® race controller can be calibrated with PSO for the considered plant model.

Related future work might involve extending the optimal calibration of the real-time Formula E® race strategy to different safety car phases and race scenarios. Moreover, the near-optimality of the proposed race strategy might be validated upon experimental data or by increasing the fidelity level for the Formula E® car plant model. In particular, a multi-fidelity simulation approach might be established in interfacing the computationally lightweight reduced-order control model with a more detailed Formula E® car plant model capable of simulating its operation within a single lap as well. Furthermore, simulating the operation of the proposed race controller in additional tracks might lay the foundations to develop dedicated design and component sizing methodologies for Formula E® car systems.

List of symbols

αSOC_{AM}	Multiplier for battery SOC depletion per lap in attack mode
αT_{AM}	Multiplier for battery temperature increase per lap in attack mode
$\alpha Time_{AM}$	Multiplier for lap time decrease in attack mode
AM	Flag for attack mode activation
BE_{lap}	Battery energy depleted throughout a single lap
$BE_{lap-min}$	Minimum battery energy depleted throughout a single lap
$BE_{lap-MAX}$	Maximum allowed battery energy depleted throughout a single lap
Δ_{SOC}	Variation in battery SOC after a single lap
Δ_{Tbatt}	Variation in battery temperature after a single lap
$\Delta_{Tbatt-rel}$	Relative variation in battery temperature after a single lap

J_{A-ECMS}	A-ECMS cost function
J_{PSO}	PSO cost function
k	Lap number
kWh_{batt}	Battery capacity
lap time	Lap time
$laps_{AM}$	Number of laps completed in a single attack mode activation
$laps_{AM-MAX}$	Maximum allowed number of laps per attack mode activation
μ_{SC}	Race cost function weighting coefficient for safety car entry
N_{lap}	Total number of laps in the e-prix
n_{AM}	Number of attack mode activations
n_{AM-MAX}	Maximum allowed number of attack mode activations
SOC	Battery state-of-charge
s_{SOC}	Equivalence factor for battery energy depletion in A-ECMS
s_T	Equivalence factor for battery temperature increase in A-ECMS
T_{batt}	Battery temperature
$T_{batt-MAX}$	Maximum allowed battery temperature
TM	Thermal mode
TM_{min}	Minimum thermal mode
TM_{MAX}	Maximum thermal mode
T_{rise}	Multiplier for battery temperature increase per lap in attack mode

References

[1] A. Emadi, "Transportation 2.0," in IEEE Power and Energy Magazine, vol. 9, no. 4, pp. 18-29, July-Aug. 2011.

[2] B. Bilgin *et al*., "Making the Case for Electrified Transportation," in *IEEE Transactions on Transportation Electrification*, vol. 1, no. 1, pp. 4-17, June 2015.

[3] K. Bayar, "Performance comparison of electric-vehicle drivetrain architectures from a vehicle dynamics perspective", *Proc. IMechE Part D: J. Automobile Engineering*, vol. 234, no. 4, pp. 915-935, 2020.

[4] P.G. Anselma, Y. Huo, J. Roeleveld, A. Emadi, G. Belingardi, "Rapid optimal design of a multimode power split hybrid electric vehicle transmission", *Proc. IMechE Part D: J. Automobile Engineering*, vol. 233, no. 3, pp. 740-762, 2019.

[5] F. Chiara, M. Canova, "A review of energy consumption, management, and recovery in automotive systems, with considerations of future trends", *Proc. IMechE Part D: J. Automobile Engineering*, vol. 227,, no. 6, pp. 914 – 936, 2013.

[6] I. Aghabali, J. Bauman, P. Kollmeyer, Y. Wang, B. Bilgin and A. Emadi, "800V Electric Vehicle Powertrains: Review and Analysis of Benefits, Challenges, and Future Trends," in *IEEE Transactions on Transportation Electrification*, in press, 2021.

[7] J. Cao and A. Emadi, "A new battery/ultra-capacitor hybrid energy storage system for electric, hybrid and plug-in hybrid electric vehicles," *2009 IEEE Vehicle Power and Propulsion Conference*, Dearborn, MI, USA, 2009, pp. 941-946.

[8] Mauduit N., Pastor G., "Venturi Formula E Team in the 100 % Electric New FIA Championship", *15. Internationales Stuttgarter Symposium*, 2015.

[9] Rizzoni G., Cooke D., Pastor G., "The fastest electric vehicles on earth: A history of electric land speed racing and of the Venturi Buckeye Bullet program", *15. Internationales Stuttgarter Symposium*, 2015.

[10] Standaert, W., Jarvenpaa, "Formula E: Next Generation Motorsport with Next Generation Fans", *International Conference on Information Systems*, 2016.

[11] Fia Formula E, "Energy Management 101: The importance of energy in Formula E", 16 March 2020, online, available: https://www.fiaformulae.com/en/news/2020/march/formula-e-energy-management (accessed 19 Feb. 2021).

[12] J. Lempert, B. Vadala, K. Arshad-Aliy, J. Roeleveld and A. Emadi, "Practical Considerations for the Implementation of Dynamic Programming for HEV Powertrains," *2018 IEEE Transportation Electrification Conference and Expo (ITEC)*, Long Beach, CA, USA, 2018, pp. 755-760.

[13] P. G. Anselma, Y. Huo, J. Roeleveld, G. Belingardi and A. Emadi, "Slope-Weighted Energy-Based Rapid Control Analysis for Hybrid Electric Vehicles," in *IEEE Transactions on Vehicular Technology*, vol. 68, no. 5, pp. 4458-4466, May 2019.

[14] W. Enang, C. Bannister, C. Brace, C. Vagg, "Modelling and heuristic control of a parallel hybrid electric vehicle", *Proc. IMechE Part D: J. Automobile Engineering*, 2015; 229(11), 1494 – 1513.

[15] P. G. Anselma, A. Biswas, J. Roeleveld, G. Belingardi and A. Emadi, "Multi-Fidelity Near-Optimal on-Line Control of a Parallel Hybrid Electric Vehicle Powertrain," *2019 IEEE Transportation Electrification Conference and Expo (ITEC)*, Detroit, MI, USA, 2019, pp. 1-6.

[16] B. Škugor, J.Deur, M.Cipek, D.Pavković, "Design of a power-split hybrid electric vehicle control system utilizing a rule-based controller and an equivalent consumption minimization strategy", *Proc. IMechE Part D: J. Automobile Engineering*, vol. 228, no. 6, pp. 631 – 648, 2014.

[17] M. Deacon, C.J. Brace, N.D. Vaughan, C.R. Burrows, R.W. Horrocks, "Impact of alternative controller strategies on exhaust emissions from an integrated diesel/continuously variable transmission powertrain", *Proc. IMechE Part D: J. Automobile Engineering*. , vol. 213, no. 2, pp. 95-107, 1999.

[18] P.K. Wong, L.M. Tam, K. Li, C.M. Vong, "Engine idle-speed system modelling and control optimization using artificial

intelligence", *Proc. IMechE Part D: J. Automobile Engineering*, vol. 224, no. 1, pp. 55-72, 2010.

[19] X. Liu and A. Fotouhi, "Formula-E race strategy development using artificial neural networks and Monte Carlo tree search", *Neural Computing and Applications*, vol. 32, pp. 15191–15207, 2020.

[20] X. Liu, A. Fotouhi and D.J. Auger, "Optimal energy management for formula-E cars with regulatory limits and thermal constraints", *Applied Energy*, vol. 279, no. 115805, 2020.

[21] X. Liu, A. Fotouhi and D.J. Auger, "Formula-E race strategy development using distributed policy gradient reinforcement learning", *Knowledge-Based Systems*, vol. 216, no. 106781, 2021.

[22] A. Heilmeier, M. Graf and M. Lienkamp, "A Race Simulation for Strategy Decisions in Circuit Motorsports," 2018 21st International Conference on Intelligent Transportation Systems (ITSC), Maui, HI, USA, 2018, pp. 2986-2993.

[23] Fia Formula E, "Attack mode: Go off the racing line and get rewarded with the power to attack. Worth the risk?", online, available: https://www.fiaformulae.com/en/championship/attack-mode (accessed 24 Feb. 2021).

[24] A. Heilmeier, M. Graf, J. Betz, M. Lienkamp, "Application of Monte Carlo Methods to Consider Probabilistic Effects in a Race Simulation for Circuit Motorsport", *Applied Sciences*, vol. 10, no. 12:4229, pp. 1-21, 2020.

[25] R. Bellman and R. Kalaba, "Dynamic programming and adaptive processes: Mathematical foundation," in *IRE Transactions on Automatic Control*, vol. AC-5, no. 1, pp. 5-10, Jan. 1960.

[26] R. Johri, Z. Filipi, "Optimal energy management of a series hybrid vehicle with combined fuel economy and low-emission objectives", *Proc. IMechE Part D: J. Automobile Engineering*, vol. 228, no. 12, pp. 1424 – 1439, 2014.

[27] J. Wang, Q.Wang, X.Zeng, P.Wang, "Research on the optimal power management strategy for a hybrid electric bus", *Proc. IMechE Part D: J. Automobile Engineering*, vol. 229, no. 11, pp. 1529 – 1542, 2014.

[28] K. van Berkel, B. de Jager, T. Hofman and M. Steinbuch, "Implementation of Dynamic Programming for Optimal Control Problems With Continuous States," in *IEEE Transactions on Control Systems Technology*, vol. 23, no. 3, pp. 1172-1179, May 2015.

[29] B. Mashadi, M. Khadem Nahvi, "Fuel consumption reduction by introducing best-mode controller for hybrid electric vehicles", *Proc. IMechE Part D: J. Automobile Engineering*, vol. 234, no. 2-3, pp. 810-821, 2020.

[30] G.Q. Ao, J.X. Qiang, H. Zhong, X.J. Mao, L. Yang, B. Zhuo, "Fuel economy and NOx emission potential investigation and trade-off of a hybrid electric vehicle based on dynamic programming", *Proc. IMechE Part D: J. Automobile Engineering*, 2008;, vol. 222, no. 10, pp. 1851-1864, 2008.

[31] V.D. Ngo, J.A. Colin Navarrete, T. Hofman, M. Steinbuch, A. Serrarens, "Optimal gear shift strategies for fuel economy and driveability", *Proc. IMechE Part D: J. Automobile Engineering*, vol. 227, no. 10, pp. 1398-1413, 2013.

[32] P. Elbert, S. Ebbesen and L. Guzzella, "Implementation of Dynamic Programming for n-Dimensional Optimal Control Problems With Final State Constraints," in *IEEE Transactions on Control Systems Technology*, vol. 21, no. 3, pp. 924-931, May 2013.

[33] O. Sundstrom, L. Guzzella, "A generic dynamic programming Matlab function", *2009 IEEE Control Applications, (CCA) & Intelligent Control, (ISIC)*, St. Petersburg, 2009, pp. 1625-1630.

[34] Fia Formula E, "Rules and regulations: the hard and fast rules of the ABB FIA Formula E Championship", online, available: https://www.fiaformulae.com/en/championship/rules-and-regulations (accessed 8 Mar. 2021).

[35] G. Paganelli, S. Delprat, T. M. Guerra, J. Rimaux and J. J. Santin, "Equivalent consumption minimization strategy for parallel hybrid powertrains," *Vehicular Technology Conference. IEEE 55th Vehicular Technology Conference. VTC Spring 2002*, Birmingham, AL, USA, 2002, pp. 2076-2081, vol.4.

[36] S. Delprat, T. M. Guerra and J. Rimaux, "Optimal control of a parallel powertrain: from global optimization to real time control strategy," *Vehicular Technology Conference. IEEE 55th Vehicular Technology Conference. VTC Spring 2002 (Cat. No.02CH37367)*, Birmingham, AL, USA, 2002, pp. 2082-2088, vol.4.

[37] S. Delprat, T. M. Guerra, G. Paganelli, J. Lauber and M. Delhom, "Control strategy optimization for an hybrid parallel powertrain," *Proceedings of the 2001 American Control Conference*, Arlington, VA, USA, 2001, pp. 1315-1320, vol.2.

[38] N. Kim, A. Rousseau, "Sufficient conditions of optimal control based on Pontryagin's minimum principle for use in hybrid electric vehicles", *Proc. IMechE Part D: J. Automobile Engineering*, vol. 226, no. 9, pp. 1160 – 1170, 2012.

[39] W. Enang, C. Bannister, "Robust proportional ECMS control of a parallel hybrid electric vehicle", *Proc. IMechE Part D: J. Automobile Engineering*, vol. 231, no. 1, pp. 99 – 119, 2016.

[40] C. Gong, M. Hu, S. Li, S. Zhan, D. Qin, "Equivalent consumption minimization strategy of hybrid electric vehicle considering the impact of driving style", *Proc. IMechE Part D: J. Automobile Engineering*, vol. 233, no. 10, pp. 2610-2623.. 2019.

[41] C. Musardo, B. Staccia, S. Bittanti, Y. Guezennec, L. Guzzella, G. Rizzoni, "An adaptive algorithm for hybrid electric vehicles energy management", *FISITA World automotive congress*, Barcelona, Spain, 2004.

[42] Y. Zhang, L. Chu, Z. Fu, et al., "An improved adaptive equivalent consumption minimization strategy for parallel plug-in hybrid electric vehicle", *Proc. IMechE Part D: J. Automobile Engineering*, vol. 233, no. 6, pp. 1649-1663, 2019.

[43] X. Lin, Q. Feng, L. Mo, H. Li, "Optimal adaptation equivalent factor of energy management strategy for plug-in CVT HEV", *Proc. IMechE Part D: J. Automobile Engineering*, vol. 233, no. 4, pp. 877-889, 2019.

[44] H. Liu, X. Li, W. Wang, L. Han, H. Xin, C. Xiang, "Adaptive equivalent consumption minimisation strategy and dynamic control allocation-based optimal power management strategy for four-wheel drive hybrid electric vehicles", *Proc. IMechE Part D: J. Automobile Engineering*, vol. 233, no. 12, pp. 3125-3146, 2019.

[45] J. Kennedy and R. Eberhart, "Particle swarm optimization," *Proceedings of ICNN'95 - International Conference on Neural Networks*, Perth, WA, Australia, 1995, pp. 1942-1948 vol.4.

[46] P.G. Anselma, G. Belingardi, "Multi-objective optimal computer-aided engineering of hydraulic brake systems for

18

electrified road vehicles", *Vehicle System Dynamics*, in press, 2021.

[47] P. Brandimarte, "Optimization Model Solving", in *An Introduction to Financial Markets: A Quantitative Approach*, USA: John Wiley & Sons Inc, 2018, pp. 717-718.

[48] M. Nouiri, A. Bekrar, A. Jemai et al., "An effective and distributed particle swarm optimization algorithm for flexible job-shop scheduling problem", *Journal of Intelligent Manufacturing*, vol. 29, no. 3, pp. 603–615, 2018.

[49] B. Mashadi, M. Khadem Nahvi, "Fuel consumption reduction by introducing best-mode controller for hybrid electric vehicles", *Proc. IMechE Part D: J. Automobile Engineering*, vol. 234, no. 2-3, pp. 810-822, 2020.

[50] Yarpiz, "Particle Swarm Optimization in MATLAB", [online] Available: https://yarpiz.com/50/ypea102-particle-swarm-optimization (accessed 10 Mar. 2021).

[51] P. Wang, J. Li, Y. Yu, X. Xiong, S. Zhao, W. Shen, "Energy management of plug-in hybrid electric vehicle based on trip characteristic prediction", *Proc. IMechE Part D: J. Automobile Engineering*, vol. 234, no. 8, pp. 2239-2259, 2020.

[52] F. Wang, X.J. Mao, B. Zhuo, H. Zhong, Z.L. Ma, "Parallel hybrid electric system energy optimization control with automated mechanical transmission", *Proc. IMechE Part D: J. Automobile Engineering*, vol. 223, no. 2, pp. 151-167, 2009.